The Physics and Modeling of Heavily Doped Emitters

JESÚS A. DEL ALAMO, STUDENT MEMBER, IEEE, AND RICHARD M. SWANSON

Abstract—The physics of minority-carrier injection and internal quantum efficiency of heavily doped emitters is studied through a novel computer simulation. It is shown that in the shallow emitters of modern devices, the transport of carriers through the bulk of the emitter, and the surface recombination rate are the dominant mechanisms controling the minority-carrier profile. Carrier recombination in the bulk of the emitter only produces a small perturbation of this profile. This observation permits us to develop a simple and accurate analytical model for the saturation current and internal quantum efficiency of shallow emitters.

I. INTRODUCTION

THE PHYSICS of heavily doped emitters has been a topic of intense research since the fabrication of diffused emitters for bipolar transistors [1]. Its importance today is not only restricted to modern polysilicon [2] or SIPOS [3], [4] emitter bipolar transistors, but it is crucial to the understanding of the open-circuit voltage of solar cells [5], and the disappearance of latchup in CMOS devices at very low temperature [6].

Considerable work has been carried out throughout the years on the physics and modeling of the minority-carrier injection into heavily doped emitters. The complexity introduced by the varying impurity profile has been treated by various methods that lead to complicated analytical solutions in terms of Bessel functions [7], [8], Taylor series expansions [9], or Hermite polynomials [10], among others. The inclusion of the bandgap narrowing that occurs in heavily doped silicon [11] and minority-carrier lifetimes that depend on the local doping level [12], [13] further complicates the modeling of practical emitters. Analytical solutions for transparent emitters [14] and more realistic emitters [5], [8], [15]–[17] are in the literature. In some cases the validity of these solutions is dependent on the physical parameters chosen to illustrate the model. In others the approximations do not have a clear physical interpretation, but are based on mathematical manipulations that simplify the solutions.

Exact computer simulations that solve the semiconductor equations for bipolar transistors or solar cells have also been used to study the complex behavior of minority carriers in heavily doped emitters [18]–[25]. These models are in general expensive to use, and their generality obscures the peculiar effects occuring inside the emitter. Other more simplified models that only solve in an exact manner the behavior of the minority carriers in the quasi-neutral portions of the emitter have been presented [26], [27]. They can provide considerable physical insight into the relevant physics of the emitter if the results are carefully interpreted. This is the approach taken in this paper.

Another relevant aspect of heavily doped emitters for solar cells and photodiodes is the internal quantum efficiency. The short-circuit current of solar cells [28] and the responsivity of photodiodes [29] specially in the UV region is controlled by the transport and recombination of photogenerated carriers in the front emitter. This important phenomena has received very little study in comparison with the dark characteristics of the emitter. Exact simulations that solve the solar cell equations include this calculation [21], [24], although detailed study of the internal quantum efficiency has not been presented. Solutions of the minority-carrier transport equations in the quasi-neutral portion of the emitter have been published [30]–[34], more with the aim of characterizing the emitter than for obtaining the internal quantum efficiency. Some highly complex analytical solutions [35], and other oversimplified analytical approximations [5], [36] are available. None of them are easily used to calculate the internal quantum efficiency of modern solar cells and photodiodes.

In this paper we study the physics of heavily doped emitters through a novel computer simulation that solves the minority-carrier transport equation in the quasi-neutral region of the emitter. The model, presented in Section III, contains significant improvements over previous models [26], [27], [30]–[34]. By making use of the super-position principle fast solutions are obtained for the emitter saturation current and the emitter internal quantum efficiency. A critical selection of physical parameters for the illustration of the model is carried out in Section II.

In Section IV the computer model is applied to several typical emitters. From the identification of the relative importance of transport, surface recombination, and bulk recombination of minority carriers, analytical models for the emitter saturation current and emitter internal quantum efficiency emerge. For the emitters in use in modern devices it is found that the recombination inside the emitter represents only a small perturbation of the minority-carrier profile of the "transparent" emitter, in which negligible bulk recombination is present. This observation leads to the development of very simple analytical models for the saturation current and internal quantum efficiency, that are also presented in Section IV. By comparison with the computer modeling the range of validity of the analytical models is found to contain most of the interesting emitters of modern bipolar transistors, solar cells, photodiodes, and CMOS devices.

Manuscript received November 1, 1983; revised June 13, 1984.

The authors are with the Stanford Electronics Laboratories, Stanford, CA 94305.

0018-9383/84/1200-1878$01.00

II. Selection of Physical Parameters

In this section we discuss the values of physical parameters selected to illustrate our emitter modeling. Since n-type heavily doped silicon has been considerably more characterized than p-type silicon because of its importance for bipolar transistors, we will limit the discussion and application of our model to n-type material.

After the Slotboom and de Graaff measurements of bandgap narrowing in p-type Si [37], most of the early work in n-type Si was unfortunately carried out in regions with variable impurity profiles [38]-[41] where the interpretation of the results is very complex. More recent experiments used As-grown material where the doping level can be considered uniform [42], [43]. In the work by Mertens *et al.* the highly As-doped substrates had impurity inhomogeneity problems, yielding erroneous results of bandgap narrowing [44], [45]. Only the three data points of Sb-doped Si are therefore selected here, together with all the data of Wieder [42] in As-doped Si.

Neugroschel *et al.* have recently measured ΔE_g from the temperature dependence of the dc emitter current of As-implanted emitters [46]. We have critically examined the assumptions that they use in their extraction of ΔE_g and we have concluded that their results are overestimated [47].

Except for two points of Mertens *et al.*, all the other data require the knowledge of the minority-carrier diffusion coefficient. Once the diffusion length is determined, or in the case of Neugroschel *et al.* the emitter thickness, the unknown quantity for the three collections of experiments is

$$\frac{n_{ie}^2 D_p}{N_D} = \frac{n_{i0}^2 D_p}{N_{D\text{eff}}} = \frac{n_{i0}^2 D_p}{N_D} \exp\left(\frac{\Delta E_g}{kT}\right) \tag{1}$$

where the symbols have their usual meaning. ΔE_g is a phenomenological bandgap narrowing, or as we have denoted somewhere else, an "apparent" or "device" bandgap narrowing [48]. It takes into account all the effects that makes n_{ie}^2 different than n_{i0}^2: band tailing due to potential fluctuations [49], rigid shrinkage of the bandgap due to many body effects [50], and degeneracy effects due to the necessity of using Fermi–Dirac statistics rather than Maxwell–Boltzmann statistics [51].

In (1), the minority-carrier diffusion coefficient must be known in order to extract ΔE_g. In the course of this work, however, we realized that the relevant parameter affecting hole transport in the bulk of shallow emitters is not ΔE_g, n_{ie}^2, or $N_{D\text{eff}}$, but $D_p \exp(\Delta E_g/kT)$, $n_{ie}^2 D_p$, or $N_{D\text{eff}}/D_p$, depending on the desired representation. Fortunately, the knowledge of D_p is not necessary for the estimation of $N_{D\text{eff}}/D_p$, which comes directly out of (1). In other words, for the type of emitters that we study here we do not need to make any assumptions about D_p, but just go back to the experimental literature and take $N_{D\text{eff}}/D_p$. We have indeed done so, and in Fig. 1 we plot $N_{D\text{eff}}/D_p$ from [42], [43], [47].

For computational convenience we now chose a given function of D_p from the majority-carrier literature [52], and find a power function for ΔE_g, so that the resulting $N_{D\text{eff}}/D_p$ gives the best fit to the results of Fig. 1. This best fit is shown in the same figure and the resulting ΔE_g algebraic expression is

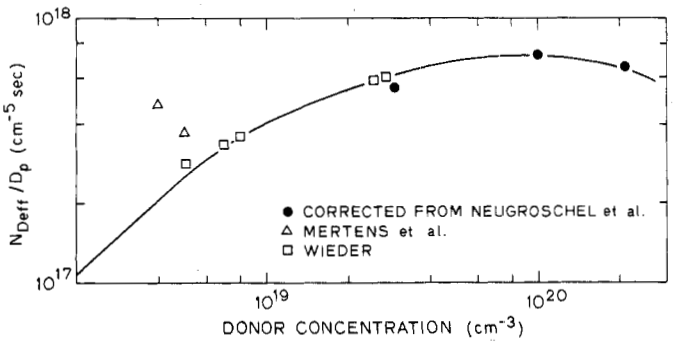

Fig. 1. Plot of experimental values of $N_{D\text{eff}}/D_p$, and curve fit used in this work (see text).

$$\Delta E_g(N_D) = 2.46 \times 10^{-6} N_D^{0.234} \text{ eV} \tag{2}$$

with N_D in cm^{-3}.

The mechanisms affecting the lifetime of minority carriers in heavily doped silicon is a subject of extensive investigation at the present. To illustrate our modeling we adopt here a pragmatic approach: we will assume the existence of two independent mechanisms controlling the hole lifetime. One of them is linearly dependent on the doping level, and the other is quadratically dependent on the doping level. The observed sensitivity of solar cell and transistor emitters to the conditions of the surface [53], [54] indicates that bulk recombination is not the dominant effect in these emitters. Our computer simulations and those of other authors [24] indicate that an Auger coefficient of the order measured by Dziewior and Schmid [55] does not support this experimental fact. Therefore, a smaller Auger coefficient [24], [56] has been chosen here. Our lifetime model is

$$\frac{1}{\tau} = 1.67 \times 10^{-12} N_D + 5 \times 10^{-32} N_D^2 \text{ s}^{-1}. \tag{3}$$

This lifetime model, like the other models presented previously in this section, only pretend to illustrate our emitter work. Further research is needed to gain a better knowledge of the minority-carrier parameters in heavily doped silicon.

III. Emitter Model

The basic one-dimensional steady-state semiconductor equations that describe the behavior of holes in a low-level injection quasi-neutral n-type region with nonuniform band structure are [57]

—the hole current equation

$$J_p = -qp\mu_p \frac{d\phi_p}{dx} \tag{4}$$

—the hole continuity equation

$$\frac{dJ_p}{dx} = q(G - U) \tag{5}$$

—and the hole density equation

$$p = p_0 \exp\frac{q\phi_p}{kT} \tag{6}$$

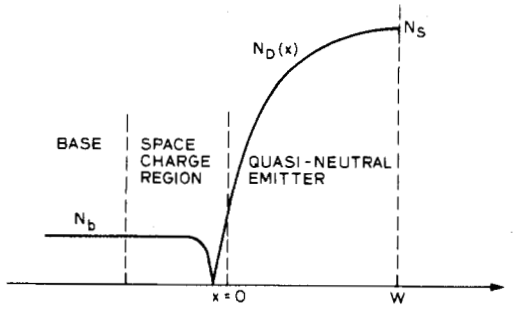

Fig. 2. Geometry of the emitter studied in this work. $X = 0$ marks the emitter edge of the space charge layer. $X = W$ is the silicon surface.

where ϕ_p is the hole quasi-fermi level measured relative to ϕ_n (the electron quasi-Fermi level), p_0 is the equilibrium hole concentration, G the hole generation rate, U the hole recombination rate, and the rest of the parameters have their usual meaning.

In this study we are going to address that portion of the emitter that is quasi-neutral (Fig. 2) where $n_0(x) \simeq N_D(x)$ [58]. Very near the metallurgical junction quasi-neutrality breaks down. For most of the voltage range, however, the current behavior of the emitter is dominated by the quasi-neutral region.

The p-n product in equilibrium, $p_0(x)\, n_0(x) = n_{ie}^2(x)$, may differ from the undoped value $n_{i0}^2(x)$ because of the factors mentioned in the previous section. With the useful definition of the effective donor concentration [11], $N_{D\text{eff}} = N_D(n_{i0}^2/n_{ie}^2)$, we can write $p_0(x)N_{D\text{eff}}(x) = n_{i0}^2$. Combining this last equation and (6) and taking the derivative, we obtain

$$\frac{d(pN_{D\text{eff}})}{dx} = pN_{D\text{eff}}\frac{q}{kT}\frac{d\phi_p}{dx}. \tag{7}$$

Introducing this result in (4) we obtain

$$J_p = -\frac{qD_p}{N_{D\text{eff}}}\frac{d(pN_{D\text{eff}})}{dx}. \tag{8}$$

Under low-injection conditions, (5) becomes

$$\frac{dJ_p}{dx} = q\left(G - \frac{p - p_0}{\tau_p}\right) \tag{9}$$

with τ_p being the hole recombination lifetime.

Equations (8) and (9) are easier to handle by defining a normalized excess electron-hole product

$$u = \frac{pN_{D\text{eff}} - p_0N_{D\text{eff}}}{n_{i0}^2} = \frac{pN_{D\text{eff}} - n_{i0}^2}{n_{i0}^2}. \tag{10}$$

They become, respectively

$$J_p = -\frac{qD_pn_{i0}^2}{N_{D\text{eff}}}\frac{du}{dx} \tag{11}$$

$$\frac{dJ_p}{dx} = qG - \frac{qn_{i0}^2}{\tau_pN_{D\text{eff}}}u. \tag{12}$$

Taking the derivative in (11) and solving for dJ_p/dx with (12) we get

$$\frac{d^2u}{dx^2} + \frac{d}{dx}\left[\ln\left(\frac{D_p}{N_{D\text{eff}}}\right)\right]\frac{du}{dx} - \frac{u}{L_p^2} = -\frac{N_{D\text{eff}}}{D_pn_{i0}^2}G \tag{13}$$

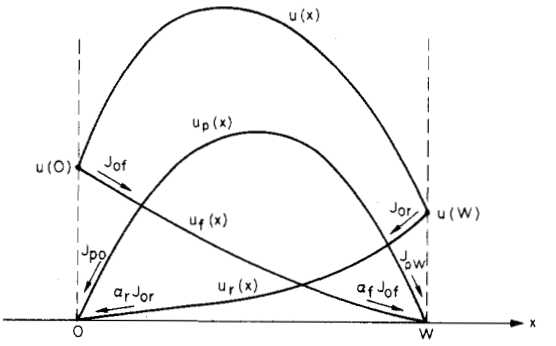

Fig. 3. Breakdown of normalized excess electron-hole product in the two solutions of the homogeneous equation of (13), and the particular solution. The indicated currents are normalized by the values of $u(x)$ at $x = 0$ and $x = W$ (see (16)).

where L_p is the local hole diffusion length. Equation (13) is a linear nonhomogeneous second-order differential equation with nonconstant coefficients. The boundary conditions are

$$u(0) = \exp\frac{q\phi_p(0)}{kT} - 1 \simeq \exp\frac{qV(0)}{kT} - 1 \tag{14a}$$

$$u(W) = \exp\frac{q\phi_p(W)}{kT} - 1 \simeq \exp\frac{qV(W)}{kT} - 1. \tag{14b}$$

The second equality is justified by the high concentration of electrons in the emitter that avoids significant deviations of the electron gas from equilibrium, so that ϕ_n is constant. $V(x)$ is the separation of quasi-Fermi levels at any point.

The general solution of (13) can be expressed as the sum of the solution to the homogeneous equation ($G = 0$), plus a particular solution. The homogeneous solution itself can be written as a linear combination of two independent solutions. We denote these solutions (within multiplying constants) $u_f(x)$, the "forward" solution, and $u_r(x)$, the "reverse" solution. The sum of the three solutions has to fulfill the boundary conditions. For convenience we take

$$u_f(0) = 1 \quad u_f(W) = 0 \tag{15a}$$

$$u_r(0) = 0 \quad u_r(W) = 1 \tag{15b}$$

$$u_p(0) = 0 \quad u_p(W) = 0 \tag{15c}$$

and the general solution can be expressed as [59]

$$u(x) = u(0)u_f(x) + u(W)u_r(x) + u_p(x) \tag{16}$$

as seen in Fig. 3. A convenient method of finding u_f, u_r, and u_p is discussed below.

We now substitute (14) and (16) into (11)

$$J_p = -qn_{i0}^2\frac{D_p}{N_{D\text{eff}}}\frac{du_f}{dx}\left[\exp\frac{qV(0)}{kT} - 1\right] - qn_{i0}^2\frac{D_p}{N_{D\text{eff}}} \cdot \frac{du_r}{dx}\left[\exp\frac{qV(W)}{kT} - 1\right] - qn_{i0}^2\frac{D_p}{N_{D\text{eff}}}\frac{du_p}{dx}. \tag{17}$$

We can now define (see Fig. 3)

$$J_{of} \triangleq -qn_{i0}^2\frac{D_p}{N_{D\text{eff}}}\frac{du_f}{dx}\bigg|_{x=0} \tag{18a}$$

$$\alpha_f J_{0f} \triangleq -qn_{i0}^2 \left.\frac{D_p}{N_{D\text{eff}}}\frac{du_f}{dx}\right|_{x=W} \tag{18b}$$

$$J_{0r} \triangleq qn_{i0}^2 \left.\frac{D_p}{N_{D\text{eff}}}\frac{du_r}{dx}\right|_{x=W} \tag{18c}$$

$$\alpha_r J_{0r} \triangleq qn_{i0}^2 \left.\frac{D_p}{N_{D\text{eff}}}\frac{du_r}{dx}\right|_{x=0} \tag{18d}$$

$$J_{p0} \triangleq qn_{i0}^2 \left.\frac{D_p}{N_{D\text{eff}}}\frac{du_p}{dx}\right|_{x=0} \tag{18e}$$

$$J_{pw} \triangleq qn_{i0}^2 \left.\frac{D_p}{N_{D\text{eff}}}\frac{du_p}{dx}\right|_{x=W} \tag{18f}$$

so that the currents at $x = 0$ and $x = W$ are

$$J_p(0) = J_{0f}\left[\exp\frac{qV(0)}{kT} - 1\right] - \alpha_r J_{0r}\left[\exp\frac{qV(W)}{kT} - 1\right] - J_{p0} \tag{19a}$$

$$J_p(W) = \alpha_f J_{0f}\left[\exp\frac{qV(0)}{kT} - 1\right] - J_{0r}\left[\exp\frac{qV(W)}{kT} - 1\right] + J_{pw}. \tag{19b}$$

With the present notation, α_f and α_r are the forward and reverse transport factors as usually defined in the base of bipolar transistors [60].

To obtain a solution to the problem, we still need to relate $V(W)$ and $V(0)$. At the surface the following relationship holds between the hole curent and the hole concentration:

$$J_p(W) = qS(p - p_0)|_{x=W} \tag{20}$$

where S is the "surface recombination velocity." The use of (10) and (14b) permits us to rewrite (20)

$$J_p(W) = J_{0s}\left[\exp\frac{qV(W)}{kT} - 1\right] \tag{21}$$

where J_{0s} is the surface saturation current

$$J_{0s} = \frac{qn_{i0}^2 S}{N_{D\text{eff}}(W)}. \tag{22}$$

Combining (21) with (19a) and (19b) we get

$$J_p(W) = \frac{J_{0s}}{J_{0s} + J_{0r}}\left\{\alpha_f J_{0f}\left[\exp\frac{qV(0)}{kT} - 1\right] + J_{pw}\right\} \tag{23}$$

$$J_p(0) = J_{0f}\frac{J_{0s} + J_{0r}(1 - \alpha_f\alpha_r)}{J_{0s} + J_{0r}}\left[\exp\frac{qV(0)}{kT} - 1\right] - \left[J_{p0} + J_{pw}\frac{\alpha_r J_{0r}}{J_{0s} + J_{0r}}\right]. \tag{24}$$

These are the most general expressions of the hole currents at the junction and at the surface of the emitter under any bias and illumination conditions.

Defining the emitter saturation current J_0 as that current flowing in the dark ($J_{p0} = J_{pw} = 0$), and the photogenerated current J_{ph} as the remaining term, (24) gives

$$J_p(0) = J_0\left[\exp\frac{qV(0)}{kT} - 1\right] - J_{ph} \tag{25}$$

where

$$J_0 = J_{0f}\frac{J_{0s} + J_{0r}(1 - \alpha_f\alpha_r)}{J_{0s} + J_{0r}} \tag{26}$$

and

$$J_{ph} = J_{p0} + J_{pw}\frac{\alpha_r J_{0r}}{J_{0s} + J_{0r}}. \tag{27}$$

It is also of interest to define an emitter transparency factor [27] in the dark, which indicates the fraction of injected carriers that recombine at the surface as opposed to recombining in the bulk.

$$\alpha_t = \left.\frac{J_p(W)}{J_p(0)}\right|_{G=0} = \frac{\alpha_f J_{0s}}{J_{0s} + J_{0r}(1 - \alpha_f\alpha_r)}. \tag{28}$$

Considering J_0 first, several cases are of practical interest:

1) If the surface recombination velocity is very large, such that $J_{0s} \gg J_{0r}$, then $J_0 \simeq J_{0f}$ and $\alpha_t \simeq \alpha_f$. This is the case of most common transistors with metal contact to the emitter and the portions of the solar cell emitter that is covered by metal [53].

2) If the surface recombination velocity is very low, such that $J_{0s} \ll J_{0r}(1 - \alpha_f\alpha_r)$, then $J_0 = J_{0f}(1 - \alpha_f\alpha_r)$. This could occur in regions of the emitter that are passivated with SiO_2.

3) If the recombination in the emitter is so high that no carriers can be transported through the emitter, it is denoted as "opaque" and $\alpha_f \simeq \alpha_r \simeq 0$. Therefore $J_0 \simeq J_{0f}$ and $\alpha_t \simeq 0$. This is the situation in the deep emitters of TPV solar cells [61] and probably in the emitters of power devices [25].

4) If all the carriers injected from one end can reach the other end of the emitter, then $\alpha_f \simeq \alpha_r \simeq 1$, $J_0 \simeq J_{0f}J_{0s}/(J_{0s} + J_{0r})$, and $\alpha_t \simeq 1$. This is the so-called "transparent" emitter characteristic of shallow emitter solar cells [62] and bipolar transistors [63], and the Al-alloyed high-low junctions of BSF solar cells [64].

In the photocurrent, as given by (27), two extreme cases are of interest to consider:

1) If the surface recombination velocity is very low, $J_{0s} \ll J_{0r}$, (27) becomes $J_{ph} \simeq J_{p0} + \alpha_r J_{pw}$. In a transparent emitter this further reduces to $J_{ph} \simeq J_{p0} + J_{pw}$ which is the maximum photogenerated current one can draw from the emitter. This is probably the case of planar photodiodes with a passivated surface, and very shallow and lightly doped emitters [65] that show quantum efficiencies very near to unity.

2) If the surface recombination velocity is very high or the transport factor is near zero because the emitter is opaque, we get $J_{ph} \simeq J_{p0}$. This is probably the case of some heavily doped deep emitters used for the characterization of lifetime in diffused layers [34].

It has been shown that in most common devices the photogenerated current in the emitter does depend very strongly on the surface treatment [32], [66], [67]. In this case, the full equation (27) needs to be used.

Denoting G_T as the total number of carriers generated inside the emitter, the internal quantum efficiency of the emitter is

$$\eta = \frac{1}{qG_T}\left(J_{p0} + J_{pw}\frac{\alpha_r J_{0r}}{J_{0s} + J_{0r}}\right). \tag{29}$$

The problem is completely solved when J_{0f}, J_{0r}, α_f, α_r, J_{p0} and J_{pw} are known for a given profile and illumination conditions. The calculation of these quantities in the most general case is done by computer by solving the coupled first-order differential equations (11) and (12). After a normalization procedure, these equations can easily be integrated. With $G = 0$ in (12) we first integrate from $x = W$ to $x = 0$ to obtain $u_f(0)$ and $J_f(0)$. The initial conditions are $u_f(W) = 0$ and an arbitrary value for $J_f(W)$. After the integration we obtain in this way a value $u_f(0)$ which in general will be different than unity. Since $J_f(0)$ is linear in $u_f(0)$, the correct J_{0f} is $J_f(0)/u_f(0)$. The forward transport factor α_f is simply $J_f(W)/J_f(0)$. We proceed in a similar way to calculate J_{0r} and α_r by integrating from $x = 0$ to $x = W$ with initial conditions $u_r(0) = 0$ and an arbitrary $J_r(0)$. We now compute J_0 and α_t from (26) and (28).

The calculation of J_{p0} and J_{pw} comes next by integrating (11) and (12) again, with the correct generation term in (12). We integrate again from $x = W$ to $x = 0$ with initial conditions $u_p(W) = 0$ and an arbitrary $J_p(W)$. At the junction ($x = 0$) we will obtain, in general, a value of $u(0)$ different than zero, and a current $J_p(0)$. Using (19a) and (19b), we can obtain

$$J_{p0} = J_{0f}\, u(0) - J_p(0) \tag{30}$$

$$J_{pw} = J_p(W) - \alpha_f J_{0f}\, u(0) \tag{31}$$

where everything is known. With all the results now we can calculate J_{ph} and η from (27) and (29). The use of linearity in the preceding manner eliminates the need to "shoot" the integration many times to obtain the desired boundary conditions.

One other interesting feature of this type of calculation is that the problem does not need to be solved again when the value of surface recombination velocity is changed. In our formalism, J_{0s} is the only expression affected by S, all the rest of the parameters coming out of the integration are constant.

IV. Results and Analytical Approximations

A computer program that solves the emitter equations as described in the previous section has been written. Although further research is needed to gain a better knowledge of the minority-carrier parameters in heavily doped silicon, the physical models selected in Section II are sufficient to illustrate the basic physics occurring in the emitters. We separately study the emitter saturation current and the internal quantum efficiency.

A. Emitter Saturation Current

Figs. 4–7 display lines of equal saturation current and transparency factor of several Gaussian emitters with different surface concentrations and junction depths for two values of surface recombination velocity $S = \infty$ and $S = 10^3$ cm/s. The base doping level is $N_b = 10^{16}$ cm^{-3}. Several distinctive domains are identifiable. We will treat them separately.

1) The "Transparent" Domain: In the previous section we identified the "transparent" emitters as those that have a transparency factor α_t of unity. This situation can appear in emitters that are either lightly doped and moderately thick, or highly doped and thin, as seen in Figs. 5 and 7. Higher values of surface recombination velocity maintain low values of excess hole

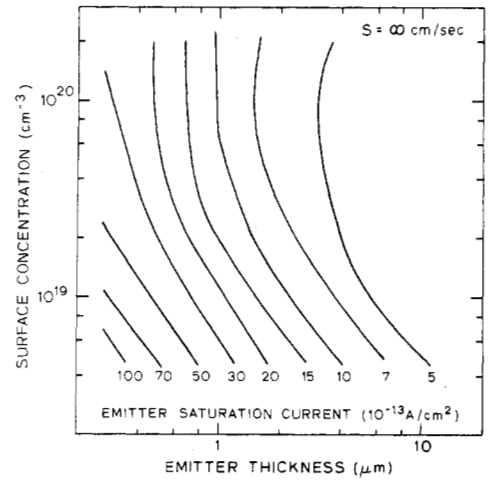

Fig. 4. Iso-saturation current lines of Gaussian n-type emitters with $S = \infty$ cm/s.

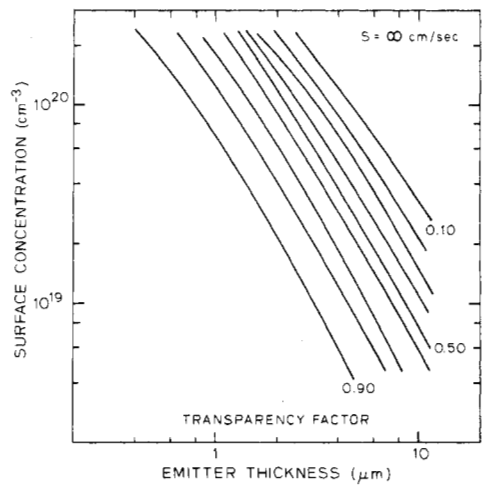

Fig. 5. Iso-transparency factor lines of Gaussian n-type emitters with $S = \infty$ cm/s.

concentration in the vicinity of the surface where the low lifetime regions exist and therefore the transparency condition is fulfilled more easily.

The modeling of these transparent emitters has already been carried out [14]. The derivation from our general formulation of Section III is straightforward and leads to the same equation as in [14]

$$J_0 = \frac{qn_{i0}^2}{\displaystyle\int_0^W \frac{N_{D\text{eff}}}{D_p}\,dx + \frac{N_{D\text{eff}}(W)}{S}}. \tag{32}$$

When the surface recombination velocity is large, the injected hole current in the emitter is limited by the transport of holes to the surface; J_0 becomes

$$J_0 = \frac{qn_{i0}^2}{G_{\text{eff}}(W)} \tag{33}$$

where

$$G_{\text{eff}}(x) = \int_0^x \frac{N_{D\text{eff}}}{D_p}\,dx \tag{34}$$

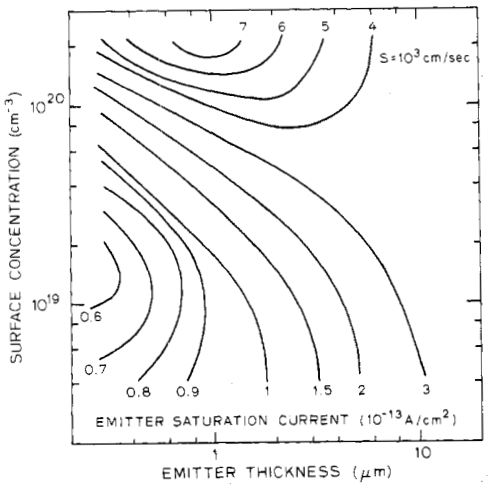

Fig. 6. Iso-saturation current lines of Gaussian n-type emitters with $S = 10^3$ cm/s.

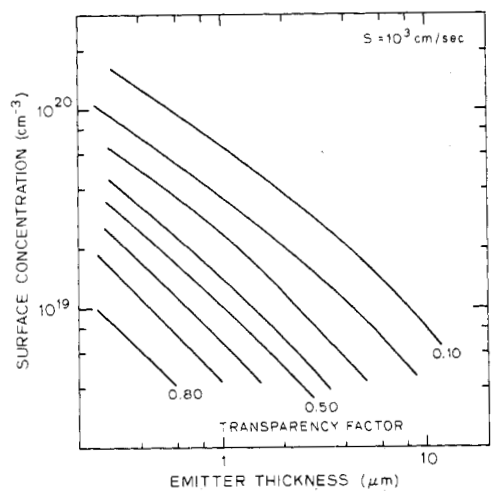

Fig. 7. Iso-transparency factor lines of Gaussian n-type emitters with $S = 10^3$ cm/s.

since it has a similar role as the Gummel number in the base of bipolar transistors [68] (except for the D_p dividing factor). We call $G_{\text{eff}}(W)$ the effective Gummel number of the emitter. To obtain the smallest J_0, the effective Gummel number of the emitter $G_{\text{eff}}(W)$ has to be maximized while the transparency of the emitter still holds. Fig. 4 indeed shows how as the surface concentration and thickness of the emitter increases, J_0 decreases.

If the surface recombination is low, the hole current may become surface recombination limited, and J_0 is

$$J_0 = \frac{qn_{i0}^2 S}{N_{D\text{eff}}(W)}. \tag{35}$$

This condition is more difficult to meet because when the surface recombination velocity is small the recombination in the bulk of the emitter is likely to be of comparable magnitude and the transparent model fails altogether. It is more likely to be fulfilled in lightly doped thin emitters where the total bulk recombination may be small, as seen in Figs. 6 and 7. In Fig. 6 we observe that at the lowest surface impurity concentrations J_0 decreases with increasing N_S. The transparency condition, however, fails very soon (see Fig. 7), and J_0 starts increasing as the bulk recombination augments.

2) The "Quasi-Transparent" Domain: As the doping level increases and the lifetime decreases, more carriers recombine within the bulk of the emitter and a smaller number reach the surface. The same effect occurs as the emitter thickness increases. The significance of bulk recombination is more pronounced and appears sooner for emitters with low surface recombination velocity. Transport limited emitters, on the other hand, are less sensitive to bulk recombination because the hole concentration in the most highly doped layers of the emitters, near the surface where the lifetime is very degraded, is very small and the hole recombination rate is therefore small too. The behavior of both types of emitters is very different. In transport limited emitters, the effect of increasing the doping level or thickness is to *reduce* J_0, while in surface recombination limited emitters J_0 *increases.*

To explain this difference we define the quasi-transparent domain as the range of emitters in which the bulk recombination is small enough so that the transparent hole distribution throughout the emitter is only slightly perturbed. With this understanding, as we increase the doping level or the thickness of transport limited emitters the holes have a higher probability of recombining because of the reduced lifetimes and longer paths. At the same time the effective Gummel number of the emitter increases. Since the first mechanism only represents a perturbation to this main limiting mechanism, J_0 decreases. This observed in Fig. 4.

In the surface recombination limited emitters the low surface recombination rate and low doping density make the hole density very high throughout the emitter. Bulk recombination increases with doping level and thickness, drawing more hole current. J_0 therefore increases.

We can now build an approximate analytical model. Integration of the continuity equation (9) (with $G = 0$) gives the emitter current as

$$J_p(0) = J_p(W) + q\int_0^W \frac{p - p_0}{\tau_p}\,dx \tag{36}$$

which is the sum of the current recombining at the surface plus the current recombining in the bulk.

Since the bulk recombination does not significantly perturb the hole distribution in the emitter, we can write

$$J_p(W) \simeq \frac{qn_{i0}^2\left(\exp\dfrac{qV(0)}{kT} - 1\right)}{G_{\text{eff}}(W) + \dfrac{N_{D\text{eff}}(W)}{S}} \tag{37}$$

and

$$(p - p_0)(x) \simeq \frac{J_p(W)}{qN_{D\text{eff}}(x)}\left[G_{\text{eff}}(W) - G_{\text{eff}}(x) + \frac{N_{D\text{eff}}(W)}{S}\right]. \tag{38}$$

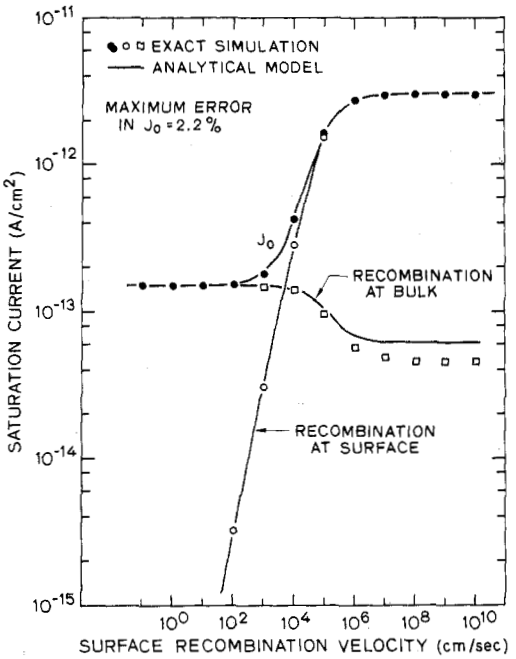

Fig. 8. Comparison of the quasi-transparent analytical emitter model results and the exact simulation for a n-type Gaussian emitter with $N_S = 10^{20}$ cm^{-3}, $W = 0.3 \times 10^{-4}$ cm, and $N_b = 10^{16}$ cm^{-3}.

The total bulk recombination current is approximately

$$q\int_0^W \frac{p-p_0}{\tau_p}\,dx \simeq J_p(W)\left[\int_0^W \frac{[G_{\text{eff}}(W)-G_{\text{eff}}(x)]\,dx}{\tau_p(x)N_{D\text{eff}}(x)} + \frac{N_{D\text{eff}}(W)}{S}\int_0^W \frac{dx}{\tau_p(x)N_{D\text{eff}}(x)}\right]. \quad (39)$$

The total emitter current is obtained by adding (37) and (39), and the saturation current becomes

$$J_0 = \frac{qn_{i0}^2}{G_{\text{eff}}(W)+\dfrac{N_{D\text{eff}}(W)}{S}}\left[1+\int_0^W \frac{[G_{\text{eff}}(W)-G_{\text{eff}}(x)]\,dx}{\tau_p(x)N_{D\text{eff}}(x)} + \frac{N_{D\text{eff}}(W)}{S}\int_0^W \frac{dx}{\tau_p(x)N_{D\text{eff}}(x)}\right] \quad (40)$$

The term in brackets in (40) provides, in effect, a first-order correction to (32) due to bulk recombination.

We have implemented (40) in an HP-41CV pocket calculator. The same physical parameters as in our full computer solution have been used. Typical results are shown in Fig. 8. The execution time required for the 2.2-percent error is 56 s. In Fig. 8 also the surface recombination component and the bulk recombination component of J_0 are separately drawn. The analytical model predicts both very well: the surface component being the first term in (40), and the bulk recombination component the other two. At very high values of S the bulk recombination component shows a greater error as compared with the computer solution. The error arises from the numerical handling of the integral in the second term of (40) in the calculator. With much smaller steps and longer execution time, this error can be reduced almost to zero. The small contribution of the bulk recombination rate in comparison with the large surface recombination gives an overall negligible error.

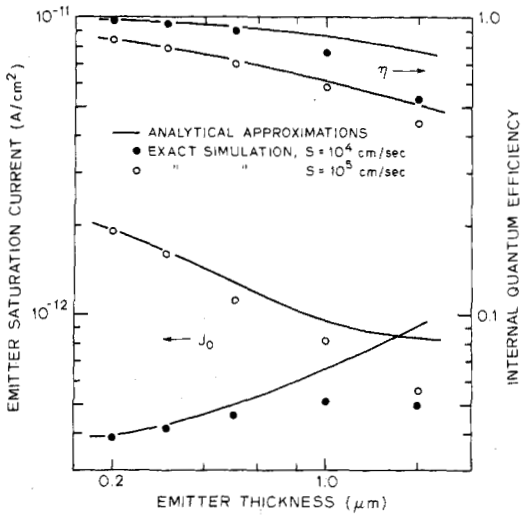

Fig. 9. Illustration of the limits of validity of the analytical approximations for a n-type Gaussian emitter, $N_S = 10^{20}$ cm^{-3}, $N_b = 10^{16}$ cm^{-3}, and variable thickness and surface recombination velocity.

Fig. 9 collects some more results in which our analytical model is compared with the computer simulation. The model breaks down as the emitter becomes opaque.

3) The "Opaque" Emitter: When the recombination in the bulk of the emitter is important very few holes reach the surface to recombine there and all of them recombine in the emitter: the emitter is "opaque" to the holes. The transparency factor becomes very near to zero. In these conditions the value of the surface recombination velocity is irrelevant.

In this case the numerical solution of Section III can be used. Alternatively a regional analysis such as that of Amantea [8] or Fossum and Shibib [17] may provide an acceptable result. Fortunately, as we have seen, most of the typical emitters used in solar cells and bipolar transistors are described by the "quasi-transparent" model, at least with the physical parameters here used. In the "opaque" category we should include the deep emitters of TPV solar cells [61], point-contact solar cells [69], and power devices [25].

B. Internal Quantum Efficiency

Fig. 10 shows the internal quantum efficiency of several Gaussian emitters with different surface concentrations and junction depths for an AM1 spectrum. The value of the surface recombination velocity is 10^3 cm/s. At low values of surface concentration and thickness the internal quantum efficiency is around unity. It drops dramatically as thickness and surface concentration increases, as has been observed experimentally for several years [28], [29], [70], [71]. Low values of surface concentration permit thick emitters without loosing to much collection, as experimentally observed by Conti *et al.* [32].

To analytically model the internal quantum efficiency we use the same theory as developed for the numerical model in

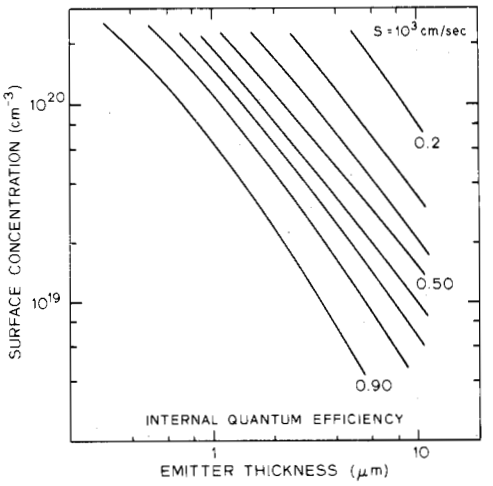

Fig. 10. Iso-internal quantum efficiency lines of Gaussian n-type emitters with $S = 10^3$ cm/s.

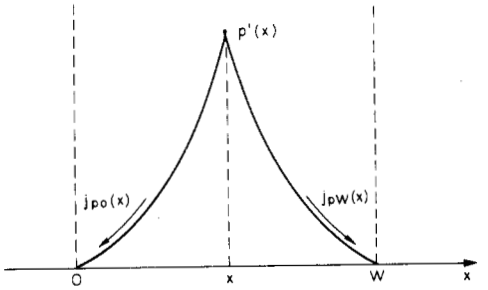

Fig. 11. Schematic of the particular solution of the minority-carrier generation profile produced by a spike of generation located at depth x (see text).

Section III. With the decomposition of the excess electron–hole product of Fig. 3 we only have to solve here for the particular solution. In the transparent case this is easily done by studying first the currents produced by a spike of generation $\delta(x)$ located at point x in the emitter that produces an excess hole concentration $p'(x)$ at that point (see Fig. 11). The currents at the surface and at the junction, in the case of zero excess carriers at those two points, are

$$j_{p0}(x) = \frac{qp'(x)N_{D\text{eff}}(x)}{G_{\text{eff}}(x)} \tag{41}$$

$$j_{pw}(x) = \frac{qp'(x)N_{D\text{eff}}(x)}{G_{\text{eff}}(W) - G_{\text{eff}}(x)}. \tag{42}$$

The total generated current is then

$$j_{p0}(x) + j_{pw}(x) = qp'(x)N_{D\text{eff}}(x)\frac{G_{\text{eff}}(W)}{G_{\text{eff}}(x)[G_{\text{eff}}(W) - G_{\text{eff}}(x)]} = q \tag{43}$$

because the integral of the δ function is 1. Therefore

$$p'(x) = \frac{[G_{\text{eff}}(W) - G_{\text{eff}}(x)]\, G_{\text{eff}}(x)}{N_{D\text{eff}}(x)G_{\text{eff}}(W)}. \tag{44}$$

For an arbitrary generation function $G(x)$, from (41) and (42) using also (44) we have the following currents:

$$J_{p0} = \int_0^W G(x)j_{p0}(x)dx = \frac{q}{G_{\text{eff}}(W)}\int_0^W G(x) \cdot [G_{\text{eff}}(W) - G_{\text{eff}}(x)]\, dx \tag{45}$$

$$J_{pw} = \int_0^W G(x)j_{pw}(x)\, dx = \frac{q}{G_{\text{eff}}(W)}\int_0^W G(x)G_{\text{eff}}(x)\, dx. \tag{46}$$

Also, from (43) we obtain

$$J_{p0} + J_{pw} = q\int_0^W G(x)\, dx = qG_T. \tag{47}$$

Now we go back to the expression of the photocurrent deduced previously (in (27)), and substitute (46) and (47) for J_{pw} and J_{p0}. Additionally we take $\alpha_r = 1$ (transparent case), J_{0s} from (22) and J_{0r} from the transparent theory. ($J_{0r} = qn_{i0}^2/G_{\text{eff}}(W)$). After some simple manipulations we get

$$J_{ph} = qG_T - \frac{q\displaystyle\int_0^W G(x)G_{\text{eff}}(x)\, dx}{G_{\text{eff}}(W) + \dfrac{N_{D\text{eff}}(W)}{S}}. \tag{48}$$

The internal quantum efficiency is therefore

$$\eta = 1 - \frac{1}{G_T}\cdot\frac{\displaystyle\int_0^W G(x)G_{\text{eff}}(x)\, dx}{G_{\text{eff}}(W) + \dfrac{N_{D\text{eff}}(W)}{S}} \tag{49}$$

which is a rigorously exact result in this case of transparent emitter. The interpretation of this equation is straightforward. If $S = 0$, then $\eta = 1$, which effectively shows that the only loss mechanism built into this model is the surface recombination. The second term in the right-hand side therefore represents the relative amount of photogenerated carriers recombining at the surface.

We have implemented (49) in the HP-41CV calculator. For the simulation of the AM1 spectrum we have chosen the integrated algebraic expression provided by Hsieh *et al.* [72]. Fig. 12 shows the comparison of the analytical expression (49) with the exact computation for a typical solar cell and photodiode emitter. Although the analytical expression (49) does not account for any bulk recombination, it predicts the internal quantum efficiency and the proportion of recombination at the surface, for all values of surface recombination velocity, with a maximum error of 1.4 percent. Similar accuracy is obtained for exponential monochromatic generation profiles, as shown in Fig. 13. The reason for this lies on the fact that high concentrations of minority carriers are never present in any part of the bulk of the emitter, even when S is very low, because the electric field aids the collection of the photogenerated carriers. The accuracy of the model improves as S increases, as seen in Fig. 13, because less carriers are in the

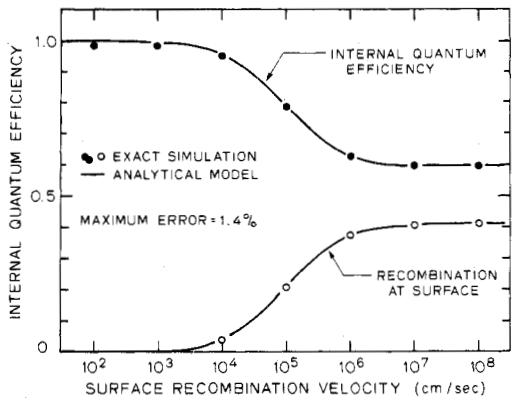

Fig. 12. Comparison of the exact solution and the transparent analytical solution for the internal quantum efficiency of an n-type Gaussian emitter with $N_S = 10^{20}$ cm^{-3}, $W = 0.3 \times 10^{-4}$ cm, and $N_b = 10^{16}$ cm^{-3}. The spectrum is AM1.

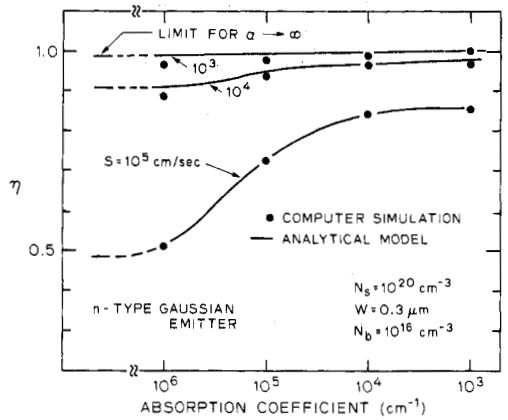

Fig. 13. Comparison of the exact solution and the transparent analytical solution for the internal quantum efficiency of an n-type emitter with the parameters indicated in the figure. The spectrum is monochromatic with the absorption coefficient in the abscissa axis.

vicinity of the highly recombining surface layers. It is interesting therefore to note that although the quasi-transparent model is necessary to describe the behavior of the emitter in the dark, a simple transparent model gives excellent accuracy when dealing with the emitter under illumination.

For monochromatic illumination of a very high α, (49) saturates at a value

$$\lim_{\alpha \to \infty} \eta = \frac{1}{1 + \dfrac{S G_{\text{eff}}(W)}{N_{D\,\text{eff}}(W)}} \tag{50}$$

which suggests a method of measuring the parameter $S/N_{D\text{eff}}(W)$ that characterizes the emitter surface recombination rate. Fig. 13 also indicates this limit.

The development of a quasi-transparent model for the internal quantum efficiency following the same chain of reasoning is straightforward. For reasons of space we have not felt the necessity of presenting it here because of the satisfactory accuracy of the transparent model in dealing with all emitters of interest for solar cells and photodiodes. As seen in Fig. 9 the domain of validity of the transparent model for the internal quantum efficiency is similar to that of the quasi-transparent model for the emitter saturation current.

V. Conclusions

A new computer simulation that simultaneously solves the saturation current and the internal quantum efficiency of quasi-neutral emitters has been developed. By using linear superposition of solutions, the calculation has been greatly sped up over previous simulations.

The physics governing the transport and recombination of minority carriers has been identified. This has permitted the development of analytical solutions for emitters in which the bulk recombination represents only a perturbation of the minority-carrier profile governed by surface recombination and bulk transport. The analytical modeling of these so-called "quasi-transparent" emitters is compared with the computer simulation, and very good accuracy is predicted for typical emitters of solar cells, bipolar transistors, and photodiodes.

The analytical models presented in this paper should be of use for the optimization of the impurity profile of shallow emitters for device applications [73].

References

[1] M. Tanenbaum and D. E. Thomas, "Diffused emitters and base silicon transistors," *Bell Syst. Tech. J.*, vol. 35, no. 1, pp. 1–22, 1956.

[2] A. A. Eltoukhy and D. J. Roulston, "The role of the interfacial layer in polysilicon emitter bipolar transistors," *IEEE Trans. Electron Devices*, vol. ED-29, no. 12, pp. 1862–1869, 1982.

[3] T. Matsushita, H. Hayashi, N. Oh-uchi, and H. Yamoto, "A SIPOS-Si heterojunction transistor," *Japan. J. Appl. Phys.*, vol. 20, suppl. 20-1, pp. 75–81, 1981.

[4] Y. H. Kwark and R. M. Swanson, "Technology and performance of SIPOS heterojunction contacts," presented at the Device Res. Conf., Fort Collins, CO, 1982.

[5] H. P. D. Lanyon, "The physics of heavily doped n^+-p junction solar cells," *Solar Cells*, vol. 3, pp. 289–311, 1981.

[6] S. Hanamura, M. Aoki, T. Masuhara, O. Minato, Y. Sakai, and T. Hayashida, "Operation of bulk CMOS devices at very low temperatures," in *Dig. 1983 Symp. VLSI Technol.* (Maui, HI), pp. 46–47, Sept. 1983.

[7] M. Klein, "Injection efficiency in double diffused transistors," *Proc. IEEE*, vol. 49, no. 11, p. 1708, 1961.

[8] R. Amantea, "A new solution for minority-carrier injection into the emitter of bipolar transistor," *IEEE Trans. Electron Devices*, vol. ED-27, no. 7, pp. 1231–1238, 1980.

[9] D. P. Kennedy and P. C. Murley, "Minority-carrier injection characteristics of the diffused emitter junction," *IEEE Trans. Electron Devices*, vol. ED-9, no. 3, pp. 136–142, 1962.

[10] W. P. Dumke, "Minority carrier injection and storage into a heavily doped emitter. Approximate solution for Auger recombination," *Solid-State Electron.*, vol. 24, pp. 155–157, 1981.

[11] H. J. J. De Man, "The influence of heavy doping on the emitter efficiency of a bipolar transistor," *IEEE Trans. Electron Devices*, vol. ED-18, no. 10, pp. 833–835, 1971.

[12] W. W. Sheng, "The effect of Auger recombination on the emitter injection efficiency of bipolar transistors," *IEEE Trans. Electron Devices*, vol. ED-22, no. 1, pp. 25–27, 1975.

[13] M. A. Shibib, F. A. Lindholm, and J. G. Fossum, "Auger recombination in heavily doped shallow-emitter silicon p-n junction solar cells, diodes, and transistors," *IEEE Trans. Electron Devices*, vol. ED-26, no. 7, pp. 1104–1106, 1979, and correction in *IEEE Trans. Electron Devices*, vol. ED-26, no. 12, p. 1978, 1979.

[14] M. A. Shibib, F. A. Lindholm, and F. Therez, "Heavily doped transparent-emitter regions in junction solar cells, diodes, and transistors," *IEEE Trans. Electron Devices*, vol. ED-26, no. 6, pp. 959–965, 1979.

[15] H. C. de Graaff, J. W. Slotboom, and A. Schmitz, "The emitter efficiency of bipolar transistors," *Solid-State Electron.*, vol. 20, pp. 515–521, 1977.

[16] C.-Y. Wu, "Current gain of the bipolar transistor," *J. Appl. Phys.*, vol. 51, no. 9, pp. 5030–5037, 1980.

[17] J. G. Fossum and M. A. Shibib, "An analytical model for minority-carrier transport in heavily doped regions of silicon devices," *IEEE Trans. Electron Devices*, vol. ED-28, no. 9, pp. 1018–1025, 1981.
[18] M. S. Mock, "On heavy doping effects and the injection efficiency of silicon transistors," *Solid-State Electron.*, vol. 17, pp. 819–824, 1974.
[19] M. S. Adler, B. A. Beatty, S. Krishna, V. A. K. Temple, and M. L. Torreno, Jr., "Limitations on injection efficiency in power devices," *IEEE Trans. Electron Devices*, vol. ED-23, no. 8, pp. 858–863, 1976.
[20] P. M. Dunbar and J. R. Hauser, "Theoretical effects of surface diffused region lifetime models on silicon solar cells," *Solid-State Electron.*, vol. 20, pp. 697–701, 1977.
[21] P. Lauwers, J. Van Meerbergen, P. Bulteel, R. Mertens, and R. J. V. Overstraeten, "Influence of bandgap narrowing on the performance of silicon n-p solar cells," *Solid-State Electron.*, vol. 21, pp. 747–752, 1978.
[22] A. Nakagawa, "One-dimensional device model of the npn bipolar transistor including heavy doping effects under Fermi statistics," *Solid-State Electron.*, vol. 22, pp. 943–949, 1979.
[23] S. P. Gaur, G. R. Srinivasan, and I. Antipov, "Verification of heavy doping parameters in semiconductor device modeling," in *IEDM Tech. Dig.*, pp. 276–279, Dec. 1980.
[24] H. T. Weaver and R. D. Nasby, "Analysis of high-efficiency silicon solar cells," *IEEE Trans. Electron Devices*, vol. ED-28, no. 5, pp. 465–472, 1981.
[25] M. S. Adler and G. E. Possin, "Achieving accuracy in transistor and thyristor modeling," *IEEE Trans. Electron Devices*, vol. ED-28, no. 9, pp. 1053–1059, 1981.
[26] R. P. Mertens, H. J. De Man, and R. J. V. Overstraeten, "Calculation of the emitter efficiency of bipolar transistors," *IEEE Trans. Electron Devices*, vol. ED-20, no. 9, pp. 772–778, 1973.
[27] J. del Alamo, J. van Meerbergen, F. D'Hoore, and J. Nijs, "High-low junctions for solar cell applications," *Solid-State Electron.*, vol. 24, pp. 533–538, 1981.
[28] J. Lindmayer, and J. F. Allison, "The violet cell: An improved silicon solar cell," *COMSAT Tech. Rev.*, vol. 3, pp. 1–21, 1973.
[29] H. Ouchi, T. Mukai, T. Kamei, and M. Okamura, "Silicon p-n junction photodiodes sensitive to ultraviolet radiation," *IEEE Trans. Electron Devices*, vol. ED-26, no. 12, pp. 1965–1969, 1979.
[30] J. Michel and A. Mircea, "Simulation de cellules solaries au silicium et comparaison avec des résultats expérimentaux," *Acta Electronica*, vol. 18, no. 4, pp. 311–330, 1975.
[31] S. G. Chamberlain, D. J. Roulston, and S. P. Desai, "Spectral response limitation mechanisms of a shallow junction n^+-p photodiode," *IEEE Trans. Electron Devices*, vol. ED-25, no. 2, pp. 241–246, 1978.
[32] M. Conti, P. Ferrari, and A. Modelli, "Recombination properties of a diffused pn junction determined by spectral response measurements," *Solid-State Electron.*, vol. 24, no. 9, pp. 879–881, 1981.
[33] C.-T. Ho, "Photovoltaic investigation of minority carrier lifetime in the heavily-doped emitter layer of silicon junction solar cell," *J. Appl. Phys.*, vol. 53, no. 1, pp. 507–513, 1982.
[34] D. J. Roulston, N. D. Arora, and S. G. Chamberlain, "Modeling and measurement of minority-carrier lifetime versus doping in diffused layers of n^+-p silicon diodes," *IEEE Trans. Electron Devices*, vol. ED-29, no. 2, pp. 284–291, 1982.
[35] J. D. Arora, S. N. Singh, and P. C. Mathur, "Surface recombination effects on the performance of n^+p step and diffused junction silicon solar cells," *Solid-State Electron.*, vol. 24, no. 8, pp. 739–747, 1981.
[36] J. Geist, "Silicon photodiode front region collection efficiency models," *J. Appl. Phys.*, vol. 51, no. 7, pp. 3993–3995, 1980.
[37] J. W. Slotboom and H. C. deGraaff, "Measurements of bandgap narrowing in Si bipolar transistors," *Solid-State Electron.*, vol. 19, pp. 857–862, 1976.
[38] H. E. J. Wulms, "Base current of I^2L transistors," *IEEE J. Solid-State Circuits*, vol. SC-12, no. 2, pp. 143–150, 1977.
[39] F. A. Lindholm, A. Neugroschel, C.-T. Sah, M. P. Godlewski, and H. W. Brandhorst, Jr., "A methodology for experimentally based determination of gap shrinkage and effective lifetimes in the emitter and base of p-n junction solar cells and other p-n junction devices," *IEEE Trans. Electron Devices*, vol. ED-24, no. 4, pp. 402–410, 1977.
[40] G. E. Possin, M. S. Adler, and B. J. Baliga, "Measurement of heavy doping parameters in silicon by electron-beam-induced current," *IEEE Trans. Electron Devices*, vol. ED-27, no. 5, pp. 983–990, 1980.
[41] D. D. Tang, "Heavy doping effects in p-n-p bipolar transistors," *IEEE Trans. Electron Devices*, vol. ED-27, no. 3, pp. 563–570, 1980.
[42] A. W. Wieder, "Emitter effects in shallow bipolar devices: Measurements and consequences," *IEEE Trans. Electron Devices*, vol. ED-27, no. 8, pp. 1402–1408, 1980.
[43] R. P. Mertens, J. L. Van Meerbergen, J. F. Nijs, and R. J. V. Overstraeten, "Measurement of the minority-carrier transport parameters in heavily doped silicon," *IEEE Trans. Electron Devices*, vol. ED-27, no. 5 pp. 949–955, 1980.
[44] R. P. Mertens, private communication, Sept. 1982.
[45] J. G. Fossum, R. P. Mertens, D. S. Lee, and J. F. Nijs, "Carrier recombination and lifetime in highly doped silicon," *Solid-State Electron.*, vol. 26, no. 6, pp. 569–576, 1983.
[46] A. Neugroschel, S. C. Pao, and F. A. Lindholm, "A method for determining energy gap narrowing in highly doped semiconductors," *IEEE Trans. Electron Devices*, vol. ED-29, no. 5, pp. 894–902, 1982.
[47] J. A. del Alamo and R. M. Swanson, "Comments on 'A method for determining energy gap narrowing in highly doped semiconductors,' " *IEEE Trans. Electron Devices*, vol. ED-31, no. 1, pp. 123–124, 1984.
[48] J. A. del Alamo, R. M. Swanson, and A. Lietoila, "Photovoltaic measurement of bandgap narrowing in moderately doped silicon," *Solid-State Electron.*, vol. 26, no. 5, pp. 483–489, 1983.
[49] E. O. Kane, "Thomas-Fermi approach to impure semiconductor band structure," *Phys. Rev.*, vol. 131, no. 1, pp. 79–88, 1963.
[50] G. D. Mahan, "Energy gap in Si and Ge: Impurity dependence," *J. Appl. Phys.*, vol. 51, no. 5, pp. 2634–2646, 1980.
[51] M. S. Lundstrom, R. J. Schwartz, and J. L. Gray, "Transport equations for the analysis of heavily doped semiconductor devices," *Solid-State Electron.*, vol. 24, pp. 195–202, 1981.
[52] N. D. Arora, J. R. Hauser, and D. J. Roulston, "Electron and hole mobilities in silicon as a function of concentration and temperatures," *IEEE Trans. Electron Devices*, vol. ED-29, no. 2, pp. 292–295, 1982.
[53] J. Nijs, F. D'Hoore, R. Mertens, and R. J. V. Overstraeten, "The dependence of the open-circuit voltage of silicon solar cells on emitter surface parameters," *Solar Cells*, vol. 6, pp. 405–418, 1982.
[54] B. Soerowirdjo and P. Ashburn, "Effects of surface treatments on the electrical characteristics of bipolar transistors with polysilicon emitters," *Solid-State Electron.*, vol. 26, no. 5, pp. 495–498, 1983.
[55] J. Dziewior and W. Schmid, "Auger coefficients for highly doped and highly excited silicon," *Appl. Phys. Lett.*, vol. 31, no. 5, pp. 346–348, 1977.
[56] G. Krieger and R. M. Swanson, "Band-to-band Auger recombination in silicon based on a tunneling technique. II. Experiment," *J. Appl. Phys.*, vol. 54, no. 6, pp. 3456–3463, 1983.
[57] K. M. van Vliet and A. H. Marshak, "The Shockley-like equations for the carrier densities and the current flows in materials with a nonuniform composition," *Solid-State Electron.*, vol. 23, pp. 49–53, 1980.
[58] J. del Alamo, "Charge neutrality in heavily doped emitters," *Appl. Phys. Lett.*, vol. 39, no. 5, pp. 435–436, 1981.
[59] A. Cuevas, A. Luque, and J. M. Ruiz, "Bifacial transcells for luminescent solar concentration," in *IEDM Tech. Dig.*, pp. 314–317, 1979.
[60] S. M. Sze, *Physics of Semiconductor Devices*. New York: Wiley, 1969, p. 304.
[61] R. M. Swanson, "Recent developments in thermophotovoltaic conversion," in *IEDM Tech. Dig.*, pp. 186–189, 1980.
[62] J. G. Fossum, F. A. Lindholm, and M. A. Shibib, "The importance of surface recombination and energy-bandgap narrowing in p-n-junction silicon solar cells," *IEEE Trans. Electron Devices*, vol. ED-26, no. 9, pp. 1294–1298, 1979.
[63] T. H. Ning and R. D. Isaac, "Effect of emitter contact on current gain of silicon bipolar devices," *IEEE Trans. Electron Devices*, vol. ED-27, n. 11, pp. 2051–2055, 1980.
[64] J. del Alamo, J. Eguren, and A. Luque, "Operating limits of Al-alloyed high-low junctions for BSF solar cells," *Solid-State Electron.*, vol. 24, pp. 415–420, 1981.
[65] F. J. Wilkinson, A. J. D. Farmer, and J. Geist, "The near ultra-

violet quantum yield of silicon," *J. Appl. Phys.*, vol. 54, no. 2, pp. 1172–1174, 1983.
[66] J. Geist, E. F. Zalewski, and A. R. Schaefer, "Spectral response self-calibration and interpolation of silicon photodiodes," *Appl. Optics*, vol. 19, no. 22, pp. 3795–3799, 1980.
[67] J. G. Fossum and E. L. Burgess, "High-efficiency p^+-n-n^+ back-surface-field silicon solar cells," *Appl. Phys. Lett.*, vol. 33, no. 3, pp. 238–240, 1978.
[68] H. K. Gummel, "A charge control relation for bipolar transistors," *Bell Syst. Tech. J.*, vol. 49, no. 1, pp. 115–120, 1970.
[69] R. M. Swanson, S. K. Beckwith, R. Crane, W. D. Eades, Y. H. Kwark, R. A. Sinton, and S. E. Swirhun, "Point-contact silicon solar cells," *IEEE Trans. Electron Devices*, vol. ED-31, no. 5, pp. 661–664, 1984.
[70] E. Y. Wang, L. Hsu, and H. W. Brandhorst, Jr., "Effects of impurity redistribution on the short-circuit current of n^+-p silicon solar cells," *J. Electrochem. Soc.*, vol. 124, no. 12, pp. 1915–1918, 1977.
[71] J. Michel and F. Lasnier, "Electrical characterization of silicon diffused layers," in *Proc. 1st European Photovoltaic Conf.* (Luxembourg), pp. 125–134, 1977.
[72] H. C. Hsieh, C. Hu, and C. I. Drowley, "A new method of analyzing the short-circuit current of silicon solar cells," *IEEE Trans. Electron Devices*, vol. ED-27, no. 4, pp. 883–885, 1980.
[73] J. del Alamo and R. M. Swanson, "Analytical modeling of heavily doped emitters for solar cells," in *Proc. 17th IEEE Photovoltaics Specialists Conf.* (Orlando, FL), to be published.

*

Jesús A. del Alamo (S'79) was born in Soria, Spain, in 1957. He received the Ingeniero Superior de Telecomunicación degree from the Universidad Politécnica de Madrid, Spain, in 1980 and the M.S. degree in electrical engineering from Stanford University, CA, in 1983. He is currently working toward the Ph.D. degree in electrical engineering at Stanford University. His Ph.D. dissertation concerns the optical and transport properties of heavily doped silicon.

From 1977 to 1981, he was a Research Assistant at the Instituto de Energía Solar of the Universidad Politécnica de Madrid. His activities there included research on the physics, modeling, and technology of bifacial monocrystalline silicon solar cells. A new solar cell was conceived by his research group that is today in production in Spain. During succesive summers he has been a Visiting Student at the following institutions: the University of Edinbourgh (U.K., 1978), Katholieke Universiteit Leuven (Belgium, 1979), and Stanford University (California, 1980).

Mr. del Alamo is a member of the Electrochemical Society and the American Physical Society. In 1980, he received the First Prize of the 1980 IEEE Region 8 Undergraduate Student Paper Contest in Stuttgart (Germany). During the summer of 1983, he was a recipient of the Electrochemical Society Energy Research Summer Fellowship Award, given by the Electrochemical Society.

*

Richard M. Swanson received the B.S.E.E. and M.S.E.E. degrees from Ohio State University, Columbus, in 1969. He received the Ph.D. degree from Stanford University, CA, in 1974.

During 1974 and 1975, he was a Research Associate at Stanford working on photovoltaics and in 1976 started his current position as Assistant Professor of Electrical Engineering at Stanford. Since then he has conducted research, along with his students, on solar cells, process-induced defects, heavy doping effects, and heterojunction contacts to silicon.

Dr. Swanson is a member of the American Physical Society, the Electrochemical Society, and the International Solar Energy Society.